



## **Explaining and predicting the increased thorax injury in aged females: age and subject-specific thorax geometry coupled with improved bone**

Downloaded from: <https://research.chalmers.se>, 2024-04-23 10:58 UTC

Citation for the original published paper (version of record):

Corrales, M., Bolte, J., Pipkorn, B. et al (2024). Explaining and predicting the increased thorax injury in aged females: age and subject-specific thorax geometry coupled with improved bone constitutive models and age-specific material properties evaluated in side impact conditions. *Frontiers in Public Health*, 12. <http://dx.doi.org/10.3389/fpubh.2024.1336518>

N.B. When citing this work, cite the original published paper.



## OPEN ACCESS

## EDITED BY

Jessica Jermakian,  
Insurance Institute for Highway Safety (IIHS),  
United States

## REVIEWED BY

Karin A. Rafaels,  
United States Army Research Laboratory,  
United States  
Sen Xiao,  
Hebei University of Technology, China

## \*CORRESPONDENCE

Duane S. Cronin  
✉ duane.cronin@uwaterloo.ca

RECEIVED 10 November 2023

ACCEPTED 05 February 2024

PUBLISHED 11 March 2024

## CITATION

Corrales MA, Bolte JH, Pipkorn B, Markusic C and Cronin DS (2024) Explaining and predicting the increased thorax injury in aged females: age and subject-specific thorax geometry coupled with improved bone constitutive models and age-specific material properties evaluated in side impact conditions. *Front. Public Health* 12:1336518. doi: 10.3389/fpubh.2024.1336518

## COPYRIGHT

© 2024 Corrales, Bolte, Pipkorn, Markusic and Cronin. This is an open-access article distributed under the terms of the [Creative Commons Attribution License \(CC BY\)](#). The use, distribution or reproduction in other forums is permitted, provided the original author(s) and the copyright owner(s) are credited and that the original publication in this journal is cited, in accordance with accepted academic practice. No use, distribution or reproduction is permitted which does not comply with these terms.

# Explaining and predicting the increased thorax injury in aged females: age and subject-specific thorax geometry coupled with improved bone constitutive models and age-specific material properties evaluated in side impact conditions

Miguel A. Corrales<sup>1</sup>, John Henry Bolte<sup>2</sup>, Bengt Pipkorn<sup>3,4</sup>, Craig Markusic<sup>5</sup> and Duane S. Cronin<sup>1\*</sup>

<sup>1</sup>Department of MME, University of Waterloo, Waterloo, ON, Canada, <sup>2</sup>Injury Biomechanics Research Center, Ohio State University, Columbus, OH, United States, <sup>3</sup>Division of Vehicle Safety, Department of Mechanics and Maritime Sciences, Chalmers University of Technology, Gothenburg, Sweden, <sup>4</sup>Autoliv Research, Vårgårda, Sweden, <sup>5</sup>Honda Development & Manufacturing of America, Raymond, OH, United States

Predicting and understanding thorax injury is fundamental for the assessment and development of safety systems to mitigate injury risk to the increasing and vulnerable aged population. While computational human models have contributed to the understanding of injury biomechanics, contemporary human body models have struggled to predict rib fractures and explain the increased incidence of injury in the aged population. The present study enhanced young and aged human body models (HBMs) by integrating a biofidelic cortical bone constitutive model and population-based bone material properties. The HBMs were evaluated using side impact sled tests assessed using chest compression and number of rib fractures. The increase in thoracic kyphosis and the associated change in rib angle with increasing age, led to increased rib torsional moment increasing the rib shear stress. Coupled with and improved cortical bone constitutive model and aged material properties, the higher resulting shear stress led to an increased number of rib fractures in the aged model. The importance of shear stress resulting from torsional load was further investigated using an isolated rib model. In contrast, HBM chest compression, a common thorax injury-associated metric, was insensitive to the aging factors studied. This study proposes an explanation for the increased incidence of thorax injury with increasing age reported in epidemiological data, and provides an enhanced understanding of human rib mechanics that will benefit assessment and design of future safety systems.

## KEYWORDS

aged population, rib fracture, thorax injury, side impact, human body model (HBM), bone constitutive modeling

## 1 Introduction

The aged adult population have demonstrated a higher mortality compared to the younger adult population (1), and the female population have a higher incidence of injury compared to the male population for similar car-crash scenarios (2). Amongst the aged population, thorax injury is the leading cause of fatalities, more so for the female population (1, 3). Importantly, female aged subjects have demonstrated a large increase in severe thorax injury for side impacts when compared to younger counterparts (3). Thorax injury has been correlated with thorax deformation (4) and rib fracture of varying severities (5). The thoracic cage load bearing tissues are the ribs, costal cartilage and sternum. It has been suggested that changes in material properties and geometry with increasing age may potentially contribute to the increased incidence of thorax injury and morbidity in the older adult population (6–8). Particular to the ribs, the cortical material properties have been measured in coupon tension testing (8). It was shown that the Young's modulus, strength (ultimate stress) and the strain to failure decreased with increasing age. Importantly, cortical bone demonstrates anisotropic behavior in coupon testing experiments with the primary direction oriented along the osteon direction (8).

Finite element human body models (HBMs) serve as crucial tools for evaluating human response and injury risk in vehicle crashes (9). However, these models are often developed for specific anthropometric, age, and sex requirements. The Global Human Body Models Consortium introduced the F05-O v5.1 detailed model (F05-O), representing a small female based on subject-specific geometry of a 26-year-old volunteer (10). The geometry was obtained through magnetic resonance imaging (MRI) and computer tomography (CT) scans of a subject reflecting the characteristics of a 5<sup>th</sup> percentile female in terms of mass, stature, and BMI. Notably, the F05-O model was developed with mesh quality requirements to ensure numerical accuracy (11). The F05-O has undergone validation in various body regions, including the thorax, with specific focus on chest compression and the incorporation of hard tissue failure using element erosion (12, 13). The material models for trabecular and cortical bone in the GHBM models are isotropic with elastic-plastic response, and simulate material failure with an element erosion criterion, based on maximum principal strain threshold.

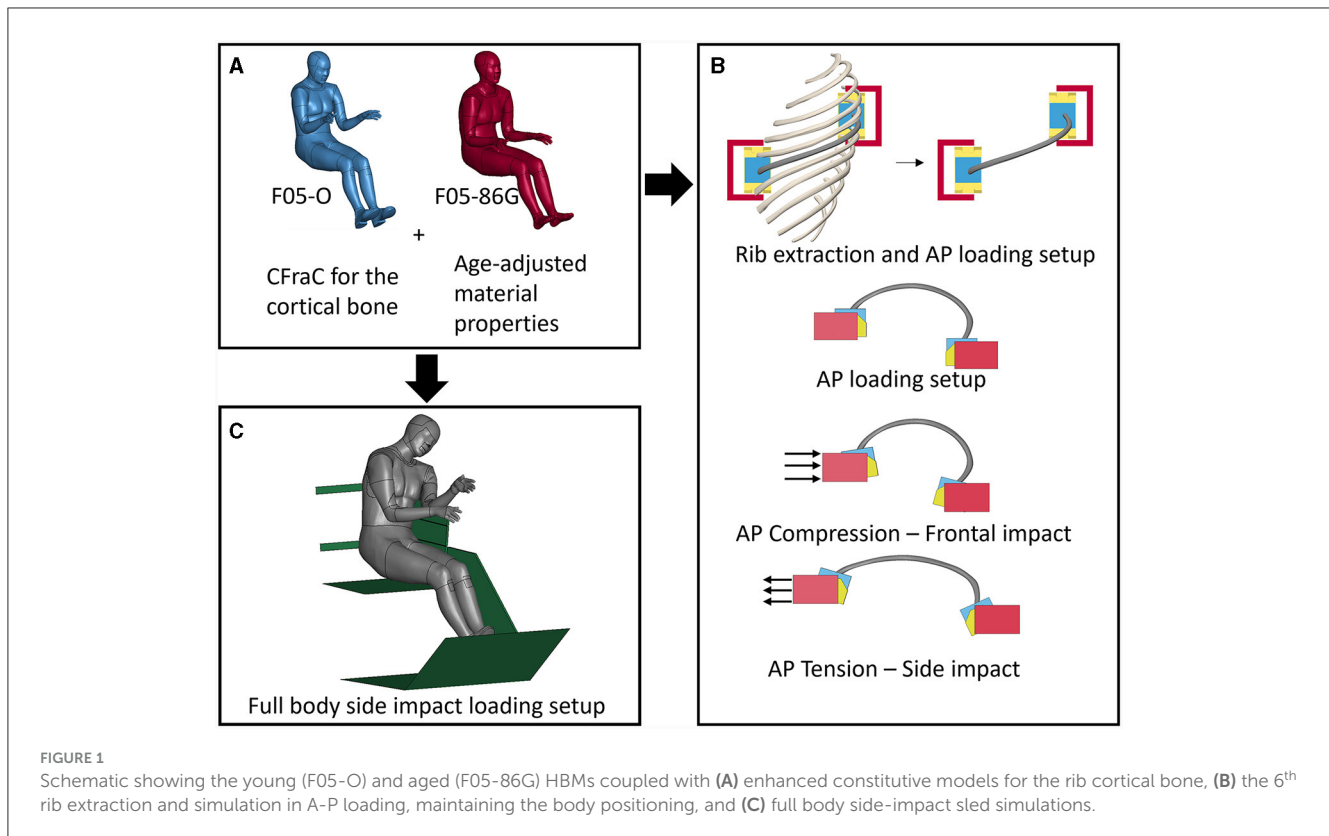
To assess the risk of thorax injury, it is important that HBM rib models predict force-displacement response, force and displacement at fracture, and fracture location in dynamic compression anterior-posterior (A-P) loading, when compared to experimental data (14). Therefore, there have been various efforts to improve rib response in compression A-P loading. A past study suggested that subject-specific rib models, based on high-resolution CT scans implemented in high density finite element mesh, could better predict rib fracture location in anterior-posterior bending, given an adequate thickness of the rib cortical cortex (15). However, such complex and computationally expensive models can be challenging to integrate in full body HBMs. A recent study (16) successfully modified a contemporary HBM rib model to better predict force-displacement response, force and displacement at fracture, and fracture location, closely matching experimental results. The improved predictions were achieved by incorporating improved biofidelic cross-sectional geometry and anisotropic and

asymmetric material models for the rib cortical and trabecular bone. Although the effect was not investigated at a full body level, the study achieved improved prediction of rib fracture and rib kinetics in an isolated rib model than can be integrated directly into full body models.

There have been various efforts to develop aged thorax models. Schoell et al. (17) specifically focused on developing a 70-year-old (YO) 50<sup>th</sup> percentile male thorax model by incorporating target geometry for the ribs and sternum based on population data; however, the thoracic kyphosis remained constant. The GHBM M50 v4.2 detailed thorax model was combined with simplified adjacent body regions, and the authors concluded that the modest geometry changes did not modify the response, while the material properties were reported to account for the changes observed between young and aged models. On the other hand, personalized full-body models have been created using global subject metrics such as mass, stature, and posture as morphing targets. These models have been used to evaluate restraint systems (18). Although these morphing targets were subject-specific, they only considered external measurements, and thus the internal geometry was not personalized. More recently, age-targeted HBM models were developed (19) by modestly modifying the rib geometry and modifying the material properties of an elastic-plastic cortical bone material model to represent the aged population. The models showed increased fracture probability with increasing age under equivalent impacts. The models were evaluated using age-adjusted injury risk curves based on cortical bone maximum principal strain. The increased injury risk found on the aged models was attributed to the changes in material properties alone and the use of age-adjusted injury risk curves, while the geometry had no effect. Recently, using a hybrid Morphing-CAD methodology, the geometry of a 26-year-old 5<sup>th</sup> percentile female model (F05-O) was morphed and repostured into an average 75-year-old (YO) and a subject-specific 86YO HBM (F05-86G) (7). This approach targeted specific bone positioning and successfully achieved precise morphing targets without compromising the mesh quality. In a simple side sled impact test, the three HBMs exhibited comparable kinematic responses but displayed distinct rib fracture patterns, with the aged models demonstrating higher number of rib fractures. However, the study did not consider changes in material properties and used elastic-plastic isotropic cortical and trabecular bone models.

A recently developed cortical bone fracture model (CFraC) (20) was proposed based on bone continuum damage mechanics with a stress triaxiality fracture criterion. The cortical bone material model and fracture criterion effectively predicted fracture initiation, location, and pattern in whole bone and specimen level tests, demonstrating consistency with the experimental data and within the population variability. Importantly, the model remained functional, accurate, and numerically stable when utilizing coarse mesh sizes commonly employed in contemporary HBMs. The CFraC model has been previously implemented in the GHBM models in isolated rib testing (16). It was concluded that including the CFraC model greatly enhanced the model's capability to predict the force and displacement at failure and fracture location.

Two human models having stature and BMI within the 5<sup>th</sup> percentile female population were investigated in this study. The



geometry for each model was subject specific. The 5<sup>th</sup> percentile female population group was investigated in this study due to the higher incidence of injury and fatality reported for small stature females compared to average stature males (1, 2, 21, 22). The young model was the GHBM 5<sup>th</sup> percentile female model, being a subject-specific scan of a 26 YO female (10). Importantly, in the context of this study, the rib angles of the GHBM 5<sup>th</sup> percentile female young model were close to the population values. In a recent study, the young model was morphed to an 84YO subject-specific geometry (7), and that aged geometry was used in the current study. The resulting rib angles for the aged geometry were higher than the population average for 84YO subjects; however, it is reported that geometric variability increases with increasing age (23).

In this study, the F05-O and the previously developed subject-specific 86-year-old small female geometry (F05-86G) model were enhanced with a recently developed cortical bone material model (Figure 1A). Then, the F05-O and the F05-86G models were enhanced with age adjusted material properties for cortical bone (F05<sub>26</sub> and F05<sub>86</sub>). The effects of geometry and material properties were investigated separately. The 6<sup>th</sup> rib was extracted from the F05-O and F05-86G models, and loaded using previously published boundary conditions (16, 24), but in a newly-proposed A-P configuration that represented the natural anatomic position of the rib (Figure 1B). The modified rib orientation allowed for the examination of geometric changes and altered posture (i.e., increased thoracic kyphosis) with increasing age using a simplified boundary condition. The extracted 6<sup>th</sup>

rib was loaded in anterior-posterior tension and compression (Figure 5) to mimic side and frontal impact rib deformation, respectively, on an isolated rib. In a side impact condition, the rib span increases (tension) due to side thorax compression. In a frontal impact condition, the rib span decreases (compression) due to the frontal thorax compression. Finally, the age-adjusted full body models were simulated in a side impact sled model (Figure 1C) and assessed based on thorax compression and predicted rib fracture.

## 2 Materials and methods

First, the F05-O and a previously developed subject-specific 86-year-old small stature female model (F05-86G) were enhanced by including recently developed material models for rib cortical bone (CFraC) (20). The CFraC model was populated with age dependent material properties from tension rib cortical bone coupon testing (8). The combination of the F05-O, F05-86G and the age dependent material properties form the various models investigated in this study (Table 1). The HBMs were evaluated in a side impact sled test (9) using chest compression as a global metric for injury assessment. In addition, the rib fracture and kinetics along the 6<sup>th</sup> rib were calculated and reported. The results of the young models were compared to those of the aged model and a factor analysis including the geometry and material properties was undertaken.

TABLE 1 Description of the geometry, material property, and constitutive model combinations investigated for the cortical bone.

Model	Description	Cortical bone material model
F05-O	Baseline GHBM C F05-O v5.1	Elastic-Plastic
F05 <sub>26</sub>	Young geometry with young material properties	CFraC
F05 <sub>26G</sub> Amp	Young geometry with aged material properties	CFraC
F05 <sub>86G</sub> Ymp	Aged geometry with young material properties	CFraC
F05 <sub>86</sub>	Aged geometry with aged material properties	CFraC

## 2.1 Enhancing the GHBM C rib fracture prediction with an age dependent cortical bone continuum damage mechanics model

The enhancement of the cortical bone material model included non-isotropic properties, meaning that the primary direction of the finite element mesh of the cortical bone (2D elements) had to be oriented along the length of the rib to match the osteon direction (8). The recently developed CFraC (20) model was used to replace the isotropic elastic-plastic material model in the F05-O. The originally published material parameters of the CFraC model were based on femur cortical bone data. In this study, the Young's modulus, ultimate stress, and strain to failure material parameters were updated using rib cortical bone coupon tension testing data (8) and implemented in the CFraC model (Figure 2).

A set of parameters for the CFraC material model to represent the older adult population was developed (Figure 2A). The effective strain vs. stress triaxiality failure criterion curve was scaled based on the strain to failure of rib cortical bone from young and aged subjects under uniaxial tension coupon testing (Figure 2B). The CFraC model parameter "C2" was modified to match the strain to failure of cortical bone coupon testing under uniaxial tension (Figure 2B).

## 2.2 Spine and local rib geometric assessment

Since two geometries were evaluated in this study and with the objective of relating differences in injury outcome to geometrical features, both the F05-O and F05-86G were geometrically evaluated. Thoracic kyphosis and local rib morphology were measured and compared between geometries (F05-O and F05-86G). The rib morphology was measured using previously reported metrics and methods concerning rib angle ( $\alpha$ PH), rib length (Sx), and location of the rib apex (Xpk) (Figure 3) (25). The measurements from the F05-O and the F05-86G were presented and compared.

## 2.3 Rib instrumentation for local rib kinetic assessment

With the objective of assessing rib kinematic response throughout the rib length, the 6<sup>th</sup> rib was instrumented in the anterior, lateral, and posterior regions. The rib kinetics were calculated in the local axis system where the "X<sub>L</sub>" axis orientation was defined by the rib length, the "Y<sub>L</sub>" axis by the primary axis of the rib cross-section, and the "Z<sub>L</sub>" axis defined by the cross product of "X<sub>L</sub>" and "Y<sub>L</sub>." The "Z<sub>L</sub>" axis was generally aligned with the secondary axis of the rib cross-section (Figure 4). The origin was defined as the central node of the rib cross-section. The primary and secondary axis of the rib cross-section (Figure 4) were calculated in the anterior, lateral and posterior regions to define the local axis systems. The three forces and the three moments were extracted from the 6<sup>th</sup> rib from the HBMs. The torsional moment (moment along X<sub>L</sub>), the bending moment (resultant moment of Z<sub>L</sub> and Y<sub>L</sub> moment), the normal force (force in the X<sub>L</sub>), and shear force (resultant force in the ZY<sub>L</sub> plane) were calculated and reported.

## 2.4 Anatomically-positioned isolated rib simulations

In a side impact, the mid-thorax (5<sup>th</sup> to 7<sup>th</sup> ribs) is primarily loaded, therefore, the 6<sup>th</sup> rib was investigated in this study for the anatomically-positioned isolated rib simulations. In addition, previous studies (15, 16) have investigated the 6<sup>th</sup> rib, allowing for direct comparison to the present study. The 6<sup>th</sup> rib was extracted from the full body models and loaded in anterior-posterior loading in tension and compression (Figure 5). In a side impact condition, the rib span increases (tension) due to side thorax compression. In a frontal impact condition, the rib span decreases (compression) due to the frontal thorax compression. Therefore, the 6<sup>th</sup> rib was loaded in AP compression and tension. The applied velocity-time curves were applied following previous experimental and computational studies (14, 16). The position of the ribs in the full body was maintained for the isolated rib simulations. The global force-displacement response, the local rib kinetic response in the anterior, lateral, and posterior regions and rib fracture location were evaluated and compared between the models.

## 2.5 Full-body side-impact simulations

The 26G and 86G models were settled in a previously published side impact sled model, representing the National Highway Traffic Safety Administration and Wayne State University designs (26, 27). The side impact sled model comprised a bench and set of rigid plates that impacted the body laterally. Ten side impact sled cases were analyzed; five HBMs (F05-O, F05<sub>26</sub>, F05<sub>26G</sub>Amp, F05<sub>86</sub>, F05<sub>86Y</sub>mp) loaded at two impact velocities. The impact velocities (3.3 m/s and 4.9 m/s) were applied to the sled while the HBMs remained unconstrained. Chest compression, rib kinetics and rib fracture were extracted from the models and compared between the models. Chest compression was defined as the change in distance between the most lateral regions of the left and right 6<sup>th</sup> ribs. In



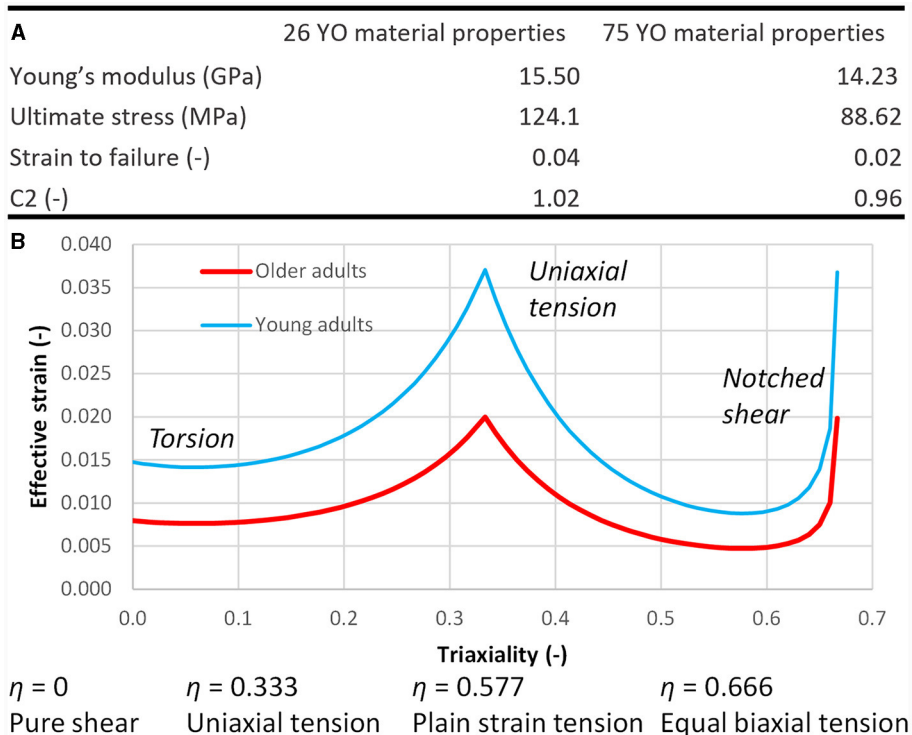


FIGURE 2

(A) Age adjusted material properties based on population experimental data (8). (B) Age adjusted effective strain-stress triaxiality curves for the CFrac constitutive model.

this study, rib fracture was defined as complete transverse element erosion in the cortical and trabecular bone of the rib.

### 3 Results

#### 3.1 Spine and local rib geometric assessment

The thoracic kyphosis of the F05-86G (48.9°) was higher when compared to that of the F05-O model (30.8°) (Figure 6A). Therefore, the rib angle ( $\alpha_{PH}$ ) (Figure 6B) was lower (from the vertical axis) (Figure 6C) for all rib levels in the F05-86G when compared to the F05-O model. The rib length ( $S_x$ ) (Figure 6C) was similar between both models. The rib apex location ( $X_{pk}$ ) (Figure 6D) varied across the rib levels; in general, the upper rib levels (1<sup>st</sup> to 7<sup>th</sup> ribs) had a more anteriorly located apex in the F05-86G model when compared to the F05-O model and more posteriorly located in the lower levels (8<sup>th</sup> to 12<sup>th</sup> ribs) when compared to the F05-O model (Figure 6E).

#### 3.2 Anatomically-positioned isolated rib simulations

When isolating the geometric effect, in both AP compression and tension, the force to failure was lower for the aged geometry (Figures 7A, B). In AP tension, the displacement to failure was

lower for the aged geometry (Figure 7A). In both compression and tension AP, the aged geometry demonstrated higher torsional moment in the location of the rib fracture (Figures 7C, D). In AP tension, the aged geometry affected the rib fracture location moving it from the posterior region in the young geometry to the anterior region in the aged geometry (Figure 7). The effect of aging material properties resulted in lower force and displacement to failure and lower torsional moment to failure maintaining the fracture location (Figure 7). The complete factorial analysis including the geometry and material properties effects on the isolated rib simulations can be found in the Appendix.

#### 3.3 Full-body side impact simulations

When assessing the models at the global level, both F05<sub>26</sub> (combined young geometry and young material properties) and F05<sub>86</sub> (combined aged geometry and aged material properties) models predicted similar lateral chest compression (Figure 8A). However, the rib fracture response varied between the young and aged models. The combined effect led to seven more rib fractures in the 3.3 m/s and eleven more rib fractures in the 4.6 m/s impact speed for the F05<sub>86</sub> model when compared to the F05<sub>26</sub> model (Figure 8B). Importantly, in the 6<sup>th</sup> rib, the aged geometry led to higher torque in the anterior and posterior rib regions (Figure 8C). The isolated effect of the geometry on rib fracture was visible at the 4.6 m/s impact severity leading to two more rib fractures in the aged geometry model (Figure 8D). The isolated effect of

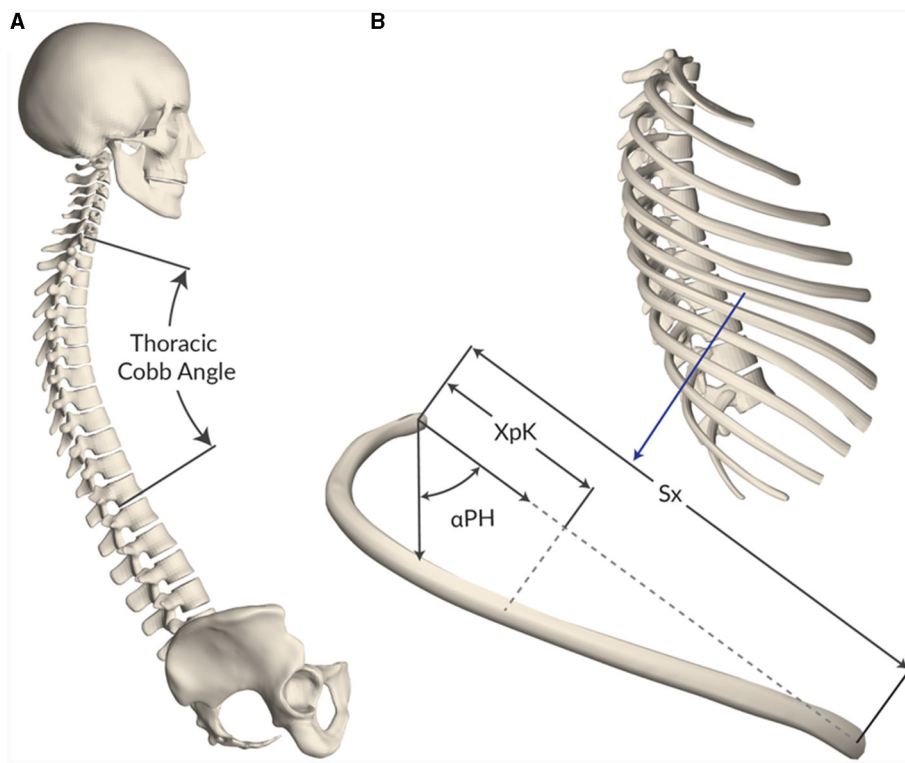


**FIGURE 3** Schematic illustrating the measured geometrical features for the F05-O and F05-86G. **(A)** For the thoracic spine, the Cobb angle was measured and compared. **(B)** For the ribs, the rib angle ( $\alpha$ PH), rib length ( $S_x$ ) and location of the rib apex ( $X_{pK}$ ) were measured and compare.

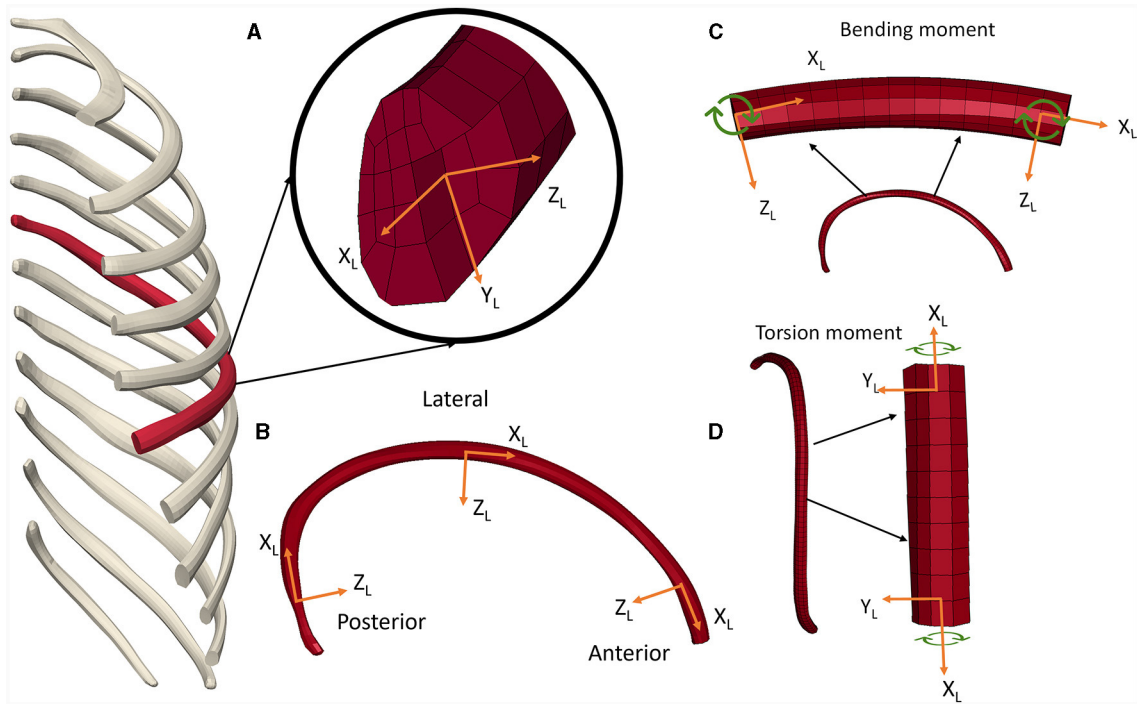
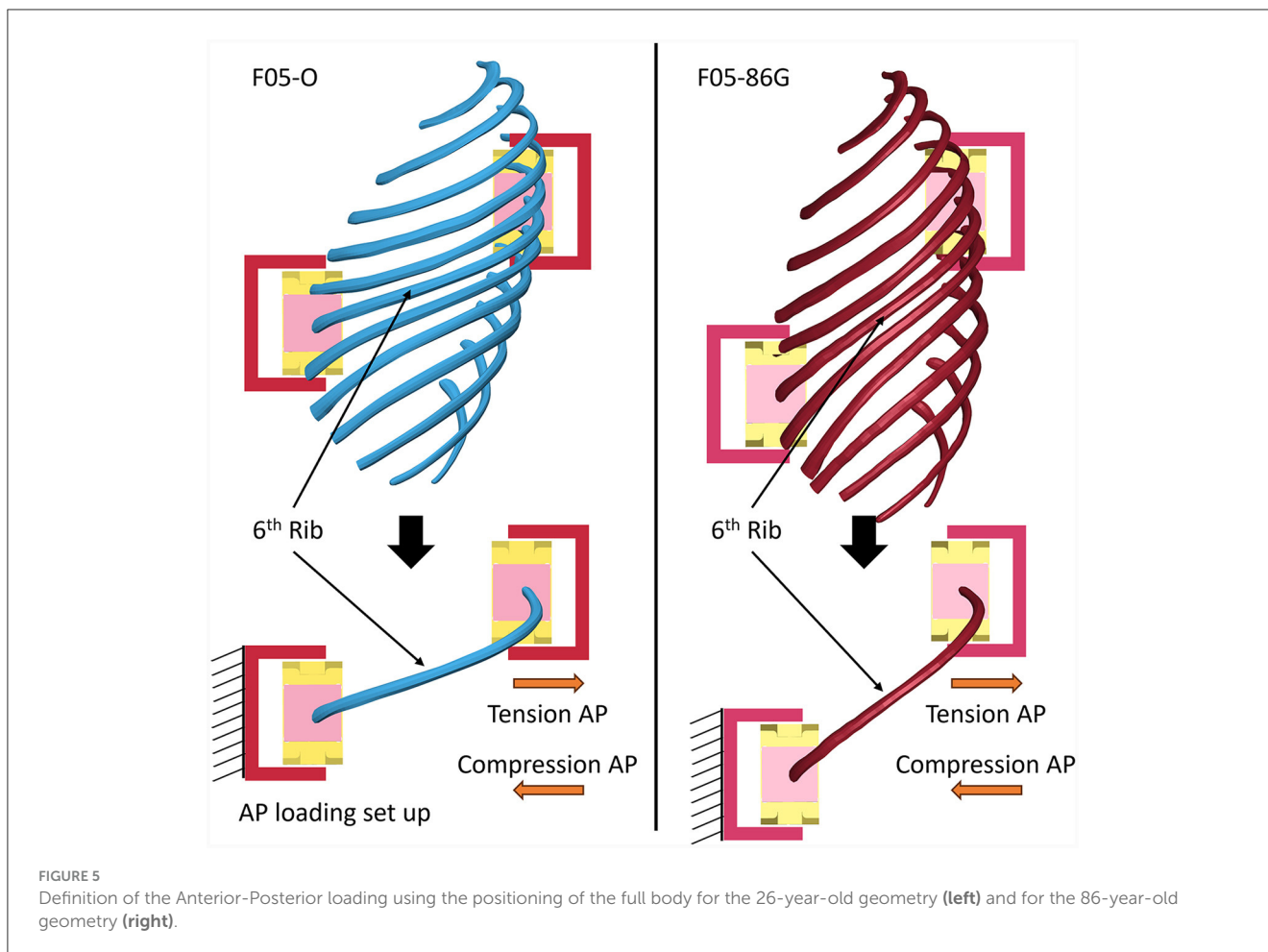


**FIGURE 4** 6<sup>th</sup> rib instrumentation for rib kinetics calculation. **(A)** Local axis system definition in **(B)** posterior, lateral and anterior rib regions. **(C)** Bending moment and **(D)** torsional moment definition.



aging the material properties on rib fracture was observed in both impact severities, with five and eight more rib fractures in the 3.3 and 4.6 m/s impact severity respectively (Figure 8F). The effect of enhancing the material models increased the number of rib fractures from zero to five in the 4.6 m/s impact severity (Figure 8E) while the effects were not apparent at lower impact severities. The factorial analysis results, including the geometry and material properties effects on the full body simulations, can be found in the Appendix.

## 4 Discussion

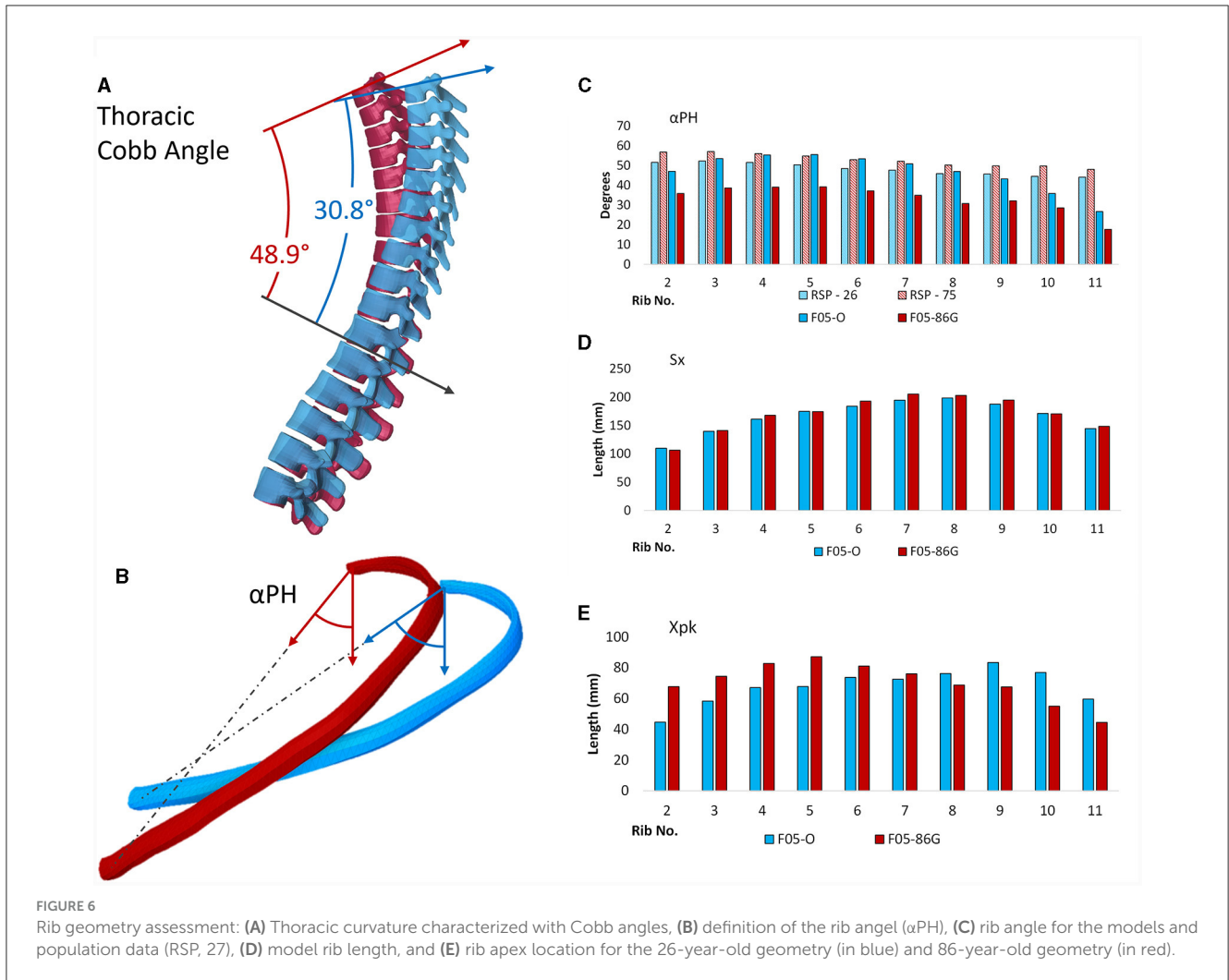
### 4.1 Geometry

Firstly, the subject-specific rib angles of the F05<sub>86</sub> model were higher (further from the horizontal) than that of the F05<sub>26</sub> model. In this study, the increased rib angle in the subject-specific aged model led to increased rib stresses and earlier failure of the ribs, with an increased number of rib fractures. It was noted that the rib angle in the subject-specific aged model was higher than the reported average for the population data (Figure 6C). The general trend in population data (28) indicates a small increase in rib angle with increasing age (Figure 6C). However, it has also been reported that population variability also increases with age

(23). This study highlights the importance of subject-specific data, with the context of average population data, aiming to capture, in part, the increasing geometrical variability with increasing age and understand the effect of such variability on thorax injury. Although population values provide an overview of geometrical changes with age at the population level, the variability associated with rib angle for a given age may also help to explain the wide range of responses that have been reported in cadaveric studies for aged subjects.

The increased kyphosis in the subject-specific model resulted in a more forward-positioned rib relative to the population. The increased kyphosis coupled with the change in rib angles affected the local rib kinetics and ultimately the rib fracture. Previous studies focusing on geometric age effects on thoracic injury have focused on modifying the rib cage with T1 and T12 as anchor points and modestly modifying the rib angles, potentially missing the full geometric effect. During the morphing process (7), it was noted that the subject-specific rib angles were not achievable if the subject-specific thoracic posture was not considered, suggesting a strong relationship between posture and rib angles. The present study accounted for the changes in thoracic kyphosis coupled with the changes in rib angle, which had not been previously explored in earlier studies, offering a novel aspect to the investigation of thorax biomechanics.





## 4.2 Anatomically-positioned isolated rib simulations

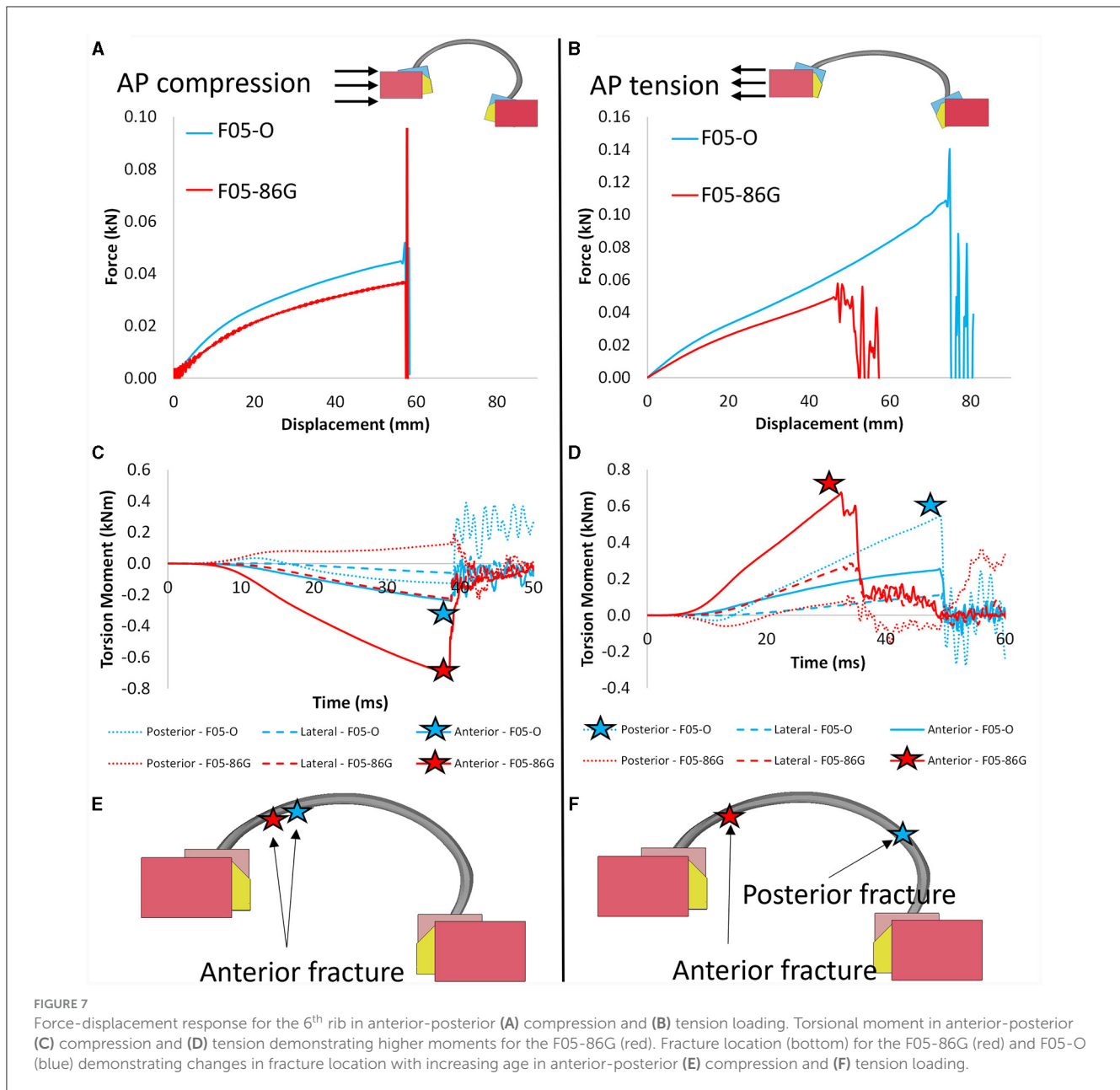
A novel anatomically-positioned anterior-posterior isolated rib loading configuration was proposed. The modified rib orientation allowed for the examination of geometric changes and altered posture (i.e., increased thoracic kyphosis) with increasing age using a simplified boundary condition. The proposed configuration provides a middle-ground between existing anterior-posterior isolated rib loading set-up and full body experiments in terms of complexity. Importantly, it proposes a loading condition that captures the effect of *in-situ* rib position which is part of the human variability. This study proposed a loading condition that isolated the effect of *in-situ* rib position, that varies in the population. In this study, it was demonstrated that accounting for the anterior-posterior position and rib angle was critical to predict rib fracture.

At the isolated rib level, a strong relationship was found between rib angle further from the horizontal and higher torsional moment. The increased torsional moment led to higher stress levels in the cortical bone, which ultimately resulted in rib failure at lower force and displacement in the aged rib than in the younger rib. This particular geometric effect highlights the crucial role of the overall

rib position (forward location in the aged geometry vs. the young geometry) and orientation (rib angle further from the horizontal) in determining the mechanical behavior of the rib structure under loading. Importantly, including an anisotropic material model with stress triaxiality fracture criteria in the models was critical to capture the geometric effect of aging included in this study. Previous research that has aimed to quantify the geometric effect of aging using a simplified material model might have underestimated the overall effect.

## 4.3 Full-body impact simulations

At the full body level, the investigation into the isolated effect of geometry demonstrated that higher torsional moments were induced due to the changes in rib angle and thoracic kyphosis, in agreement with the outcomes of isolated rib simulations. Moreover, the geometric effect also led to a higher number of rib fractures, suggesting an important role of geometry in determining the response of the aged population to impacts. In this study, exhaustive geometric aging of the model was carried out, encompassing overall posture, rib angles, and morphology leading



to increased number of rib fractures. This comprehensive approach stands in contrast to previous studies that modestly account for aging in the geometry and suggested that the geometry played a modest role in the increased injury risk for the aged population.

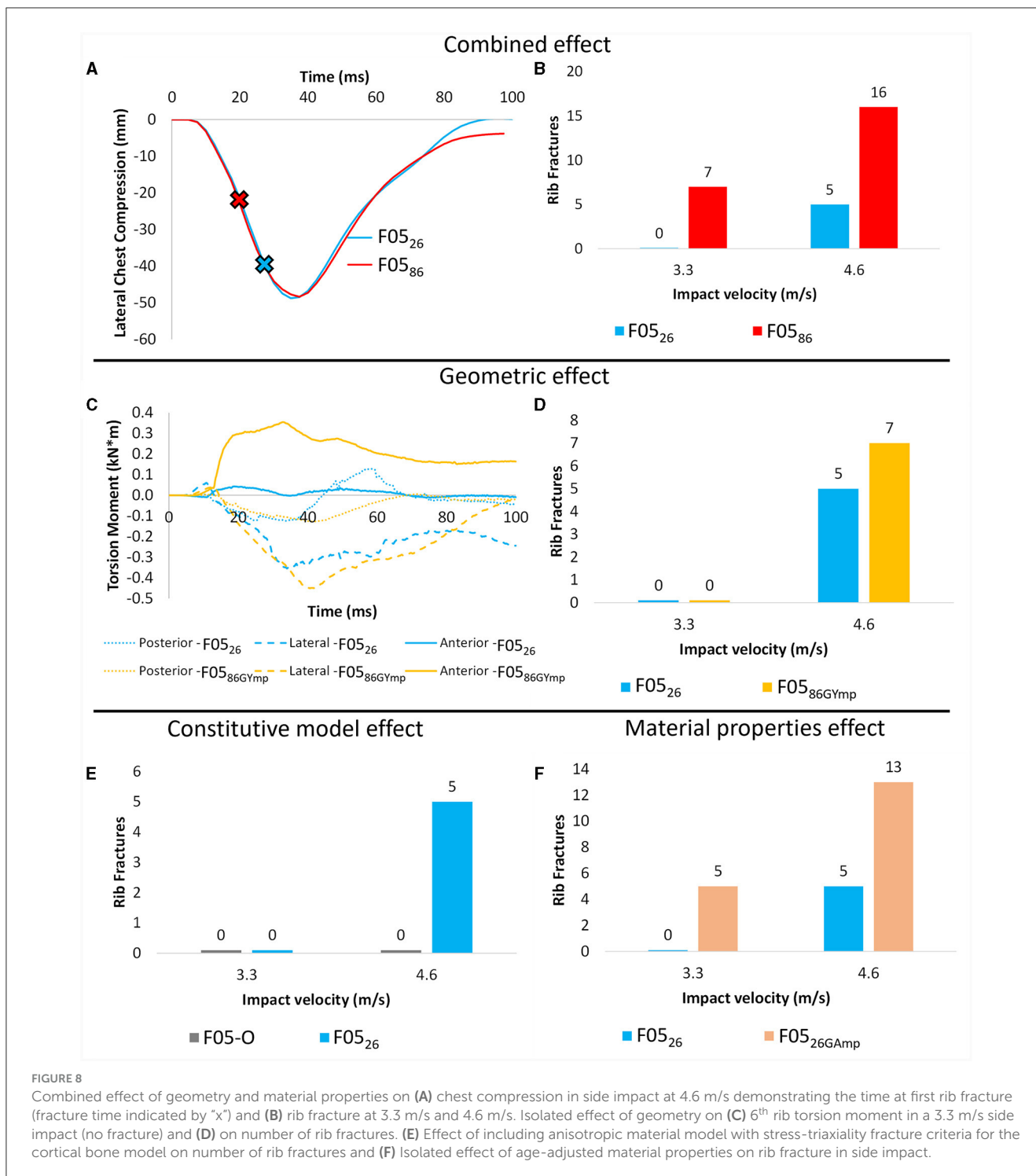
Furthermore, the aging of material properties emerged as the primary factor influencing the number of rib fractures, with its impact being further amplified by the geometric factors included in this study. These findings emphasize the importance of considering both factors, material properties, and geometry, when investigating the biomechanical response of the aged population. Such integrated analyses are vital for a more accurate understanding of injury risk and response in older individuals, contributing to the improvement of safety measures and injury prevention strategies tailored to this specific demographic.

#### 4.4 Limitations

First, only side impact was considered in the present study. Epidemiology indicates that frontal impact is an important condition to consider when evaluating chest injury. Future work will investigate the models in a frontal impact configuration.

This work included subject-specific geometries and population data for the material properties. To the author's knowledge, the relationship between age-related changes in geometry and material properties is unknown. Future research to understand the relationship, if any, between changing geometry and material properties with age.

In this study, cortical bone was investigated due to the structural relevance of the cortical bone being higher than that



of the trabecular bone (29–31). It is acknowledged that trabecular bone properties and aging effects (6) can also contribute to rib response and will be investigated in future studies. Similarly, cortical bone thickness was not altered in the present study. Exploring the impact of cortical bone thickness changes associated with aging in future research may yield additional information on its role in age-related thorax injuries and fractures.

In this study, version 5.1 of the GHBM F05-O detailed model was used. Although there have been improvements in

other body regions in the more recent versions of the GHBM model, this study focused on the ribs and the effect of rib angle, thoracic kyphosis, and rib cortical bone material properties on thorax response and injury. An advanced constitutive model for cortical bone was implemented, which contributed to explaining the difference in injury risk between young and aged subjects.

Lastly, the study did not consider changes in cross-sectional area due to aging. Addressing these areas of research in the future would contribute to a more comprehensive assessment of bone

aging effects and their implications for the biomechanical response and injury risk in the aged population.

## 4.5 Conclusions

By incorporating biofidelic material models, the HBMs were able to demonstrate sensitivity to the combined effects of rib angle and age-adjusted material properties. The current study highlights the importance of using biofidelic material models that accurately represent the material response in parametric studies. Using simplified material models (e.g., isotropic) and fracture criteria (e.g., metals plasticity) could overlook important factors in response and injury risk.

Accounting for age-related changes in overall posture, including thorax curvature, rib angles and rib morphology, proved essential in predicting higher rib fractures for the aged models. Increasing rib angle from horizontal, particularly in the aged model, led to higher rib torsional moments (and higher stress in the cortical bone), contributing to the increased number of rib fractures observed in the aged model. Importantly, the subject-specific rib angles were only achievable if the subject-specific thoracic curvature was considered. The present findings suggest that, considering overall posture and rib angles when studying age-related thoracic biomechanics is important, as these factors are coupled and play a critical role in the injury outcome.

The loading of a single rib in anterior-posterior (AP) loading, maintaining the anatomical rib angle, isolates the geometric factors considered in this study in a simplified load case. The present study showed that the position in the rib, relative to the loading (e.g., rib angle), played a strong role in the rib mechanical response. In particular, the isolated rib simulations demonstrated the importance of torsion in leading to earlier rib fracture, generated by offset loads due to rib angle. The proposed simplified loading set-up can be used in future work aimed at investigating rib mechanics accounting for the rib body positioning.

The present study showed that the total number of rib fractures, time at fracture, and rib local kinetics have a high sensitivity to rib angle and age-adjusted cortical bone material properties. Higher rib angles (further from the horizontal) led to higher stresses, including torsional stresses on the rib for the aged model, demonstrating an important difference between the young and aged models. In contrast, chest compression demonstrated no change between the young and aged models investigated. The lack of sensitivity may be due to the measured chest deflection including local rib deflection as well as gross chest deformation, and the location of the measurement points. The outcome of this study suggests that other metrics outside of chest compression may be necessary when assessing injury risk for aged people.

## Data availability statement

The original contributions presented in the study are included in the article/[Supplementary material](#), further inquiries can be directed to the corresponding author.

## Author contributions

MC: Conceptualization, Data curation, Formal analysis, Investigation, Methodology, Software, Validation, Visualization, Writing—original draft, Writing—review & editing. JB: Funding acquisition, Resources, Supervision, Writing—review & editing. BP: Funding acquisition, Resources, Supervision, Writing—review & editing. CM: Funding acquisition, Resources, Supervision, Writing—review & editing. DC: Conceptualization, Data curation, Formal analysis, Funding acquisition, Investigation, Methodology, Project administration, Resources, Software, Supervision, Validation, Visualization, Writing—review & editing.

## Funding

The author(s) declare financial support was received for the research, authorship, and/or publication of this article. This study was funded by Honda R&D Americas and the Natural Sciences and Engineering Research Council of Canada, the Global Human Body Model Consortium for use of the HBM, Compute Canada for computational resources, and Autoliv and the Ohio State University for the use of the subject-specific data. This research was undertaken, in part, thanks to funding from the Canada Research Chairs Program. The authors declare that this study received funding from Honda Development & Manufacturing of America, Ohio, USA and Autoliv Research, Vårgårda, Sweden. The funders Honda Development & Manufacturing of America and Autoliv Research were not involved in the study design, collection, analysis, interpretation of data, the writing of this article, or the decision to submit it for publication.

## Conflict of interest

BP was employed by Autoliv Research. CM was employed by Honda Development & Manufacturing of America.

The remaining authors declare that the research was conducted in the absence of any commercial or financial relationships that could be construed as a potential conflict of interest.

## Publisher's note

All claims expressed in this article are solely those of the authors and do not necessarily represent those of their affiliated organizations, or those of the publisher, the editors and the reviewers. Any product that may be evaluated in this article, or claim that may be made by its manufacturer, is not guaranteed or endorsed by the publisher.

## Supplementary material

The Supplementary Material for this article can be found online at: <https://www.frontiersin.org/articles/10.3389/fpubh.2024.1336518/full#supplementary-material>

## References

- Kahane JC. *Injury vulnerability and effectiveness of occupant protection technologies for older occupants and women*. National Highway Traffic Safety Administration. Report No. DOT HS 811 766. (2013).
- Forman J, Poplin GS, Shaw CG, McMurry TL, Schmidt K, Ash J, et al. Automobile injury trends in the contemporary fleet: belted occupants in frontal collisions. *Traffic Inj Prev.* (2019) 20:607–12. doi: 10.1080/15389588.2019.1630825
- Ramachandran R, Kashikar T, Bolte J. Injury patterns of elderly occupants involved in side crashes. In: *Conference proceedings International Research Council on the Biomechanics of Injury, IRCOBI* (2017).
- Schmitt KU, Niederer P, Muser M, Walz F. Trauma biomechanics. In: *Trauma Biomechanics*. (Berlin: Springer) (2019). doi: 10.1007/978-3-030-11659-0
- Gennarelli T, Woodzin E. *Abbreviated Injury Scale: 2015 Revision (6 ed.)*. Washington, DC: Association for the Advancement of Automotive Medicine. (2018).
- Albert DL, Katzenberger MJ, Hunter RL, Agnew AM, Kemper AR. Effects of loading rate, age, and morphology on the material properties of human rib trabecular bone. *J Biomech.* (2023) 156:111670. doi: 10.1016/j.jbiomech.2023.111670
- Corrales MA, Bolte J, Malcolm S, Pipkorn B, Cronin DS. Methodology to geometrically age human body models to average and subject-specific anthropometrics, demonstrated using a small stature female model assessed in a side impact. *Comput Methods Biomech Biomed Engin.* (2022) 26:1208–19. doi: 10.1080/10255842.2022.2112187
- Katzenberger MJ, Albert DL, Agnew AM, Kemper AR. Effects of sex, age, and two loading rates on the tensile material properties of human rib cortical bone. *J Mech Behav Biomed Mater.* (2020) 102:103410. doi: 10.1016/j.jmbbm.2019.103410
- Gierczycka D, Cronin D. Importance of impact boundary conditions and pre-crash arm position for the prediction of thoracic response to pendulum, side sled, and near side vehicle impacts. *Comput Methods Biomech Biomed Engin.* (2021) 24:1531–44. doi: 10.1080/10255842.2021.1900132
- Davis ML, Allen BC, Geer CP, Stitzel JD, Gayzik FS. A multi-modality image set for the development of a 5th percentile female finite element model. In: *IRCOBI Conference Proceedings*. (2014).
- Corrales MA, Cronin DS. Sex, age and stature affects neck biomechanical responses in frontal and rear impacts assessed using finite element head and neck models. *Front Bioeng Biotechnol.* (2021) 9:681134. doi: 10.3389/fbioe.2021.681134
- Li Z, Kindig MW, Kerrigan JR, Untaroiu CD, Subit D, Crandall JR, et al. Rib fractures under anterior-posterior dynamic loads: experimental and finite-element study. *J Biomech.* (2010) 43:228–34. doi: 10.1016/j.jbiomech.2009.08.040
- Zeng W, Mukherjee S, Caudillo A, Forman J, Panzer MB. Evaluation and validation of thorax model responses: a hierarchical approach to achieve high biofidelity for thoracic musculoskeletal system. *Front Bioeng Biotechnol.* (2021) 9:712656. doi: 10.3389/fbioe.2021.712656
- Kang YS, Kwon HJ, Stammen J, Moorhouse K, Agnew AM. Biomechanical response targets of adult human ribs in frontal impacts. *Ann Biomed Eng.* (2021) 49:900–11. doi: 10.1007/s10439-020-02613-x
- Iraeus J, Lundin L, Storm S, Agnew A, Kang Y-S, Kemper A, et al. Detailed subject-specific FE rib modeling for fracture prediction. *Traffic Inj Prev.* (2019) 20:S88–95. doi: 10.1080/15389588.2019.1665649
- Rampersadh C, Agnew AM, Malcolm S, Gierczycka D, Iraeus J, Cronin D. Factors affecting the numerical response and fracture location of the GHBM M50 rib in dynamic anterior-posterior loading. *J Mech Behav Biomed Mater.* (2022) 136:105527. doi: 10.1016/j.jmbbm.2022.105527
- Schoell SL, Weaver AA, Vavalle NA, Stitzel JD. Age- and sex-specific thorax finite element model development and simulation. *Traffic Inj Prev.* (2015) 16:S57–65. doi: 10.1080/15389588.2015.1005208
- Piqueras A, Pipkorn B, Iraeus J, Maza-Frechín M, López-Valdés FJ. Assessment of in situ chest deflection of post mortem human subjects (PMHS) and personalized human body models (HBM) in nearside oblique impacts. *Traffic Inj Prev.* (2022) 23:181–6. doi: 10.1080/15389588.2022.2036731
- von Kleeck BW, Hostetler Z, Fleischmann K, Weaver AA, Gayzik FS. Age targeted human body models indicate increased thoracic injury risk with aging. *Traffic Inj Prev.* (2022) 23:S74–9. doi: 10.1080/15389588.2022.2097223
- Cronin DS, Watson B, Khor F, Gierczycka D, Malcolm S. Cortical bone continuum damage mechanics constitutive model with stress triaxiality criterion to predict fracture initiation and pattern. *Front Bioeng Biotechnol.* (2022) 10:1022506. doi: 10.3389/fbioe.2022.1022506
- Frankel VH, Nordin M. Biomechanics of bone. *Basic Biomech Musculoskel Syst.* (2001) 3:26–59.
- Cullinane DM, Einhorn TA. Biomechanics of bone. In: *Principles of Bone Biology*. Academic Press (2002). p. 17–32. doi: 10.1016/B978-012098652-1/50104-9
- Klinich KD, Ebert SM, Reed MP. Quantifying cervical-spine curvature using bézier splines. *J Biomech Eng.* (2012) 134:114503. doi: 10.1115/1.4007749
- Agnew AM, Schafman M, Moorhouse K, White SE, Kang YS. The effect of age on the structural properties of human ribs. *J Mech Behav Biomed Mater.* (2015) 41:302–14. doi: 10.1016/j.jmbbm.2014.09.002
- Holcombe SA, Wang SC, Grotberg JB. The effect of age and demographics on rib shape. *J Anat.* (2017) 231:229–47. doi: 10.1111/joa.12632
- Cavanaugh JM, Walilko TJ, Malhotra A, Zhu Y, King AI. Biomechanical response and injury tolerance of the thorax in twelve sled side impacts. *SAE Trans.* (1990) 99:1678–93. doi: 10.4271/902307
- Pintar FA, Yoganandan N, Hines MH, Maltese MR, McFadden J, Saul R, et al. Chestband analysis of human tolerance to side impact. *SAE Trans.* (1997) 106:3612–23. doi: 10.4271/973320
- Holcombe SA, Wang SC, Grotberg JB. Age-related changes in thoracic skeletal geometry of elderly females. *Traffic Inj Prev.* (2017) 18:S122–8. doi: 10.1080/15389588.2017.1309526
- Osterhoff G, Morgan EF, Shefelbine SJ, Karim L, McNamara LM, Augat P. Bone mechanical properties and changes with osteoporosis. *Injury.* (2016) 47:S11–20. doi: 10.1016/S0020-1383(16)47003-8
- Carter DR, Hayes WC. Compact bone fatigue damage: a microscopic examination. *Clin Orthop Relat Res.* (1977) 113:265–74. doi: 10.1097/00003086-197709000-00039
- Nordin M, Frankel VH, editors. *Basic Biomechanics of the Musculoskeletal System*. Lippincott Williams & Wilkins (2001).